# Precision tools for the simulation of double-Higgs production via vector-boson fusion

# Barbara Jäger,<sup>a</sup> Alexander Karlberg,<sup>b</sup> Simon Reinhardt<sup>a</sup>

ABSTRACT: We present two precision tools for the simulation of Higgs-pair production via vector-boson fusion in the kappa framework for the parameterization of non-standard Higgs couplings. A new implementation of the process is developed in the framework of the POWHEG BOX program that can be used to provide predictions at the next-to-leading order (NLO) of QCD matched to parton showers (PS). In addition, the existing provBFHH program for the computation of next-to-next-to-leading order (NNLO) QCD and next-to-next-to-leading order QCD corrections is extended to account for values of the Higgs couplings different from the expectation of the Standard Model. We systematically compare and analyse predictions obtained with the two programs and find that the NLO+PS predictions provide a good approximation of the NNLO results for observables of the tagging jets and Higgs bosons. The results turn out to be very sensitive to the values of the modified Higgs couplings. Finally we study the non-factorizable NNLO QCD corrections to the process in the presence of anomalous couplings. We find that the size of the non-factorizable corrections is very sensitive to the anomalous couplings.

KEYWORDS: QCD, Parton Shower, NLO, Matching, Higgs

For the purpose of Open Access, the authors have applied a CC BY public copyright licence to any Author Accepted Manuscript (AAM) version arising from this submission.

<sup>&</sup>lt;sup>a</sup> Institute for Theoretical Physics, University of Tübingen, Auf der Morgenstelle 14, 72076 Tübingen, Germany

<sup>&</sup>lt;sup>b</sup>CERN, Theoretical Physics Department, CH-1211 Geneva 23, Switzerland

C	$\mathbf{onte}$	nts	
1	Inti	1	
2	Details of the implementation		
	2.1	Extension of provBFHH	4
	2.2	Implementation in the POWHEG BOX	6
3	Phenomenological results		7
	3.1	Setup	7
	3.2	Parton-shower matched results	9
	3.3	Hadronization and underlying event	12
	3.4	Impact of anomalous couplings	12
		$3.4.1$ Inclusive results at $N^3LO$	15
		3.4.2 Impact on non-factorizable corrections	16
4	Cor	nclusions and outlook	17

#### 1 Introduction

After the discovery of the Higgs boson by the ATLAS [1] and CMS [2] experiments at the CERN Large Hadron Collider (LHC) in 2012 Higgs physics has entered a precision era. The production of a Higgs boson as predicted by the Standard Model (SM) has been measured in various production modes. No significant indications for physics beyond the SM (BSM) have been identified, and all measurements so far are compatible with the spin-zero, CP-even nature of the SM Higgs boson. To learn more about the nature of this particle, a determination of the Higgs self couplings remains to be achieved, as these are intimately related to the shape of the Higgs potential. Such measurements are ideally performed in processes involving the pair production of two Higgs bosons. While the largest production rates are expected for the inclusive Higgs pair production process that predominantly proceeds via gluon fusion, the purely electroweak (EW) vector-boson fusion (VBF) channel,  $pp \rightarrow HH + 2$  jets, exhibits smaller production rates yet better means for a selection of signal events via the characteristic tagging jets that accompany the Higgs bosons in the final state. A quantitative understanding of this channel is thus as important as are flexible tools that can be used in experimental analyses and phenomenological studies.

The ATLAS and CMS experiments have performed a series of searches for Higgs-pair production both in inclusive setups and in the VBF channel (see [3, 4] for recent combinations of experimental results), deriving bounds on the triple Higgs coupling  $g_{HHH}$  as well as the quartic Higgs-to-weak boson coupling  $g_{HHVV}$ . All results are so far compatible with

the SM predictions. Due to the low production cross section Higgs pair production has yet to be discovered at the LHC, but it is expected to be so at the upcoming HL-LHC.

The relevance of the VBF HH process for a determination of the triple Higgs coupling was first discussed in [5], and its sensitivity to the quartic HHVV coupling was explored in [6]. In the past there has also been interest in studying the sensitivity of the VBF HHprocess to specific scenarios beyond the SM [7–9], and the discriminating power of VBF versus the gluon fusion background has been studied in Refs. [10, 11]. The next-to-leading order (NLO) QCD corrections to the SM process are available in the parton-level Monte-Carlo program VBFNLO [5, 12–14], and the NLO corrections have also been studied in the context of the two-Higgs doublet model [15], and in [16] using Higgs Effective Field Theory for double and triple Higgs production via VBF. NLO-QCD results matched to a parton shower (PS) as obtained with the multi-purpose program MadGraph5\_aMC@NLO [17] have first been presented in [18]. The leading factorizable next-to-next-to-leading order (NNLO) QCD corrections for Higgs pair production via VBF were presented for inclusive predictions in Ref. [19]. The fully differential predictions at this order were since computed using the projection-to-Born method [20, 21] and complemented by the inclusive next-tonext-to-next-to-leading order (N<sup>3</sup>LO) QCD calculation in [22]. While the NNLO-QCD corrections were found to be significant in some regions of phase space, yet higher orders of QCD were found to be very small. NLO-EW corrections, on the other hand, can be quite pronounced in some kinematic regions [23]. Non-factorizable corrections that are colour-suppressed but formally of the same order in the strong coupling as the dominant factorizable NNLO-QCD corrections have been found to be negligible after selection cuts typical for VBF measurements [24].

The QCD corrections of Refs. [21, 22, 24] have been implemented in the public proVBFHH program, available from https://github.com/alexanderkarlberg/proVBFH together with the proVBFH program [20, 25] for the related VBF single Higgs production process.

In this article we will explore the impact of QCD corrections and PS effects on observables of immediate relevance for the extraction of the triple Higgs and the HHVV coupling from measurements of the VBF HH process. To this end we present a new and public implementation of the VBF HH process in the POWHEG BOX [26], a tool for the matching of NLO-QCD corrections with PS generators using the POWHEG formalism [27, 28]. In order to facilitate a comparison of predictions with existing experimental results we have also implemented the so-called kappa framework [29, 30] which accounts for new physics effects in the Higgs couplings in a generic way. These couplings have also been fully implemented in the provberh program, providing predictions with modified couplings up to N³LO in the QCD coupling. The anomalous couplings have been implemented in both the factorizable and non-factorizable corrections in provberh. Besides providing very fast inclusive cross section predictions the program was also used to cross-check our POWHEG BOX implementation.

To analyse the capabilities of our new POWHEG BOX implementation we present two studies. First, we provide predictions at NLO+PS accuracy with a number of widely used parton showers, namely PYTHIA8 [31], Vincia [32] and HERWIG7 [33], and compare them to the fixed-order NNLO-QCD predictions. We stress that although NLO+PS predictions

for the VBF HH process can in principle be obtained with MadGraph5\_aMC@NLO, it can at the moment only be reliably matched to HERWIG7 as has been observed for other VBF processes [34, 35]. Our work therefore overcomes an important obstruction in obtaining NLO accurate predictions matched to the widely used PYTHIA8-family of showers. In general we find that the NLO+PS predictions provide a reasonable approximation of the NNLO-QCD predictions for inclusive observables.

Secondly we compute predictions at NLO+PS with modified Higgs couplings for a number of distributions. Using values of the couplings consistent with current experimental bounds show huge distortions compared to the SM, highlighting the sensitivity of the VBF HH channel to these couplings.

Finally we study for the first time the interplay between anomalous couplings and the higher order QCD corrections. In particular we find that the non-factorizable corrections are extremely sensitive to the anomalous corrections, and that enhancements of up to 40% can be found for even small coupling modifications. The factorizable corrections on the other hand are almost completely independent of the anomalous couplings, as expected.

The paper is structured as follows: We provide some details on the respective calculations and tools in Sec. 2 and then present phenomenological results in Sec. 3. Finally we conclude in Sec. 4.

# 2 Details of the implementation

EW Higgs pair production in association with two jets involves two types of contributions: First, VBF topologies that are dominated by the scattering of two (anti-)quarks via the tchannel exchange of massive weak gauge bosons that subsequently emit two Higgs bosons. Second, Higgs-strahlung contributions that are due to the annihilation of a quark-antiquark pair resulting in an s-channel weak gauge boson that subsequently results in an on-shell Higgs pair and a weak boson further decaying hadronically. While VBF- and Higgs-strahlung topologies contribute to HH+2 jets final states at the same order  $\alpha^4$ in the electroweak coupling, they give rise to very different kinematic features of the jets. This can be exploited to experimentally extract samples dominated by either topology. In particular, VBF events are characterized by two so-called tagging jets in the forward and backward regions of the detector with large rapidity separation,  $y_{jj}^{\text{tag}}$ , and invariant mass,  $m_{ij}^{\text{tag}}$ . When selection cuts typical for VBF analyses at the LHC are imposed, the contribution of non-VBF topologies to the EW HH+2 jets fiducial cross section was found to be at the sub-percent level [23]. In this work we will thus focus on the VBF production mode. For our new POWHEG BOX calculation we will furthermore assume that contributions involving colour exchange between upper and lower fermion lines in the VBF contributions are negligible. Within this VBF approximation QCD corrections to upper and lower quark lines decouple. The validity of this factorized approximation has been verified at percentlevel in Ref. [24]. When neglecting Higgs-strahlung contributions it is furthermore exact at NLO-QCD.

While the VBF-induced single Higgs production process has already been extensively explored at the LHC, Higgs pair production is more difficult to access due to the small

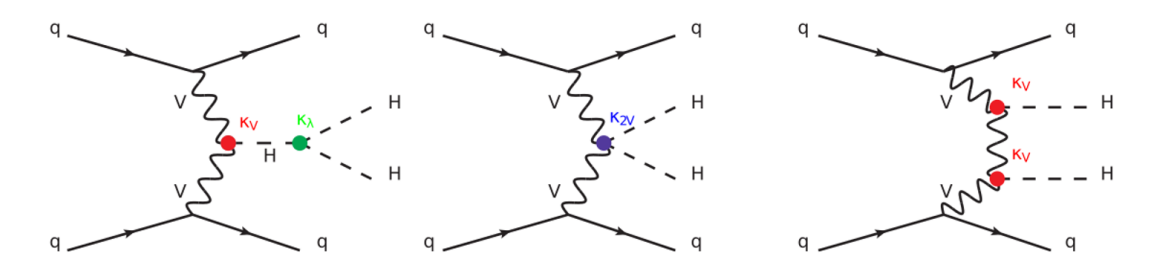


Figure 1: Representative Feynman diagrams contributing to VBF HH production.

associated cross section. However, the VBF HH process is of prime relevance for a determination of Higgs couplings that cannot be accessed at tree level in single-Higgs production processes, in particular the trilinear Higgs coupling,  $g_{HHH}$ , and the quartic coupling  $g_{HHVV}$  between Higgs and massive weak bosons  $V = W^{\pm}, Z$ . A simple prescription to parameterize deviations from the SM, the so-called kappa framework, has been suggested in [29, 30]. Within this framework a coupling modifier  $\kappa_i$  is defined as the ratio of a coupling  $c_i$  to the corresponding SM value  $c_i^{\rm SM}$ . In particular, we will express couplings of the Higgs boson entering the VBF-induced HH + 2 jets process as

$$g_{HHH} = \kappa_{\lambda} \cdot g_{HHH}^{\text{SM}}, \quad g_{HHVV} = \kappa_{2V} \cdot g_{HHVV}^{\text{SM}}, \quad g_{HVV} = \kappa_{V} \cdot g_{HVV}^{\text{SM}}.$$
 (2.1)

Here,  $g_{HVV}$  denotes the trilinear coupling of a Higgs boson to two massive weak bosons. In contrast to  $g_{HHH}$  and  $g_{HHVV}$  this coupling is accessible in single-Higgs production processes. However, it also enters the VBF-induced Higgs-pair production process via diagrams where a single Higgs boson couples to two weak bosons exchanged in the t-channel and thus appears in our calculation. Representative LO Feynman diagrams with anomalous couplings are shown in Fig. 1.

While the kappa framework does not constitute a fully unitarised extension of the SM, it is often applied in experimental analyses because of its simplicity. To allow experimentalists to nonetheless take advantage of tools providing predictions of high accuracy, we have extended the inclusive version of the provBFHH program to account for non-SM values of  $\kappa_{\lambda}$ ,  $\kappa_{2V}$ ,  $\kappa_{V}$ . Additionally, we have prepared an implementation of the VBF HH process in the context of the POWHEG BOX V2 (which we will just call the POWHEG BOX in the rest of the paper) that also offers the option for non-SM values of the above-mentioned Higgs couplings. We stress that these two implementations are completely independent, the POWHEG BOX relying on matrix elements and provBFHH on structure functions, and that the agreement between the codes therefore provides a very strong cross-check.

We will discuss the extension of the provBFHH program and the new POWHEG BOX implementation below.

#### 2.1 Extension of proVBFHH

The provBFHH program [21, 22, 24] is a tool for the computation of NNLO- and N<sup>3</sup>LO-QCD corrections to VBF HH production using the VBF approximation. From v1.1.0 it can also provide non-factorizable corrections in the eikonal approximation. At NNLO it is

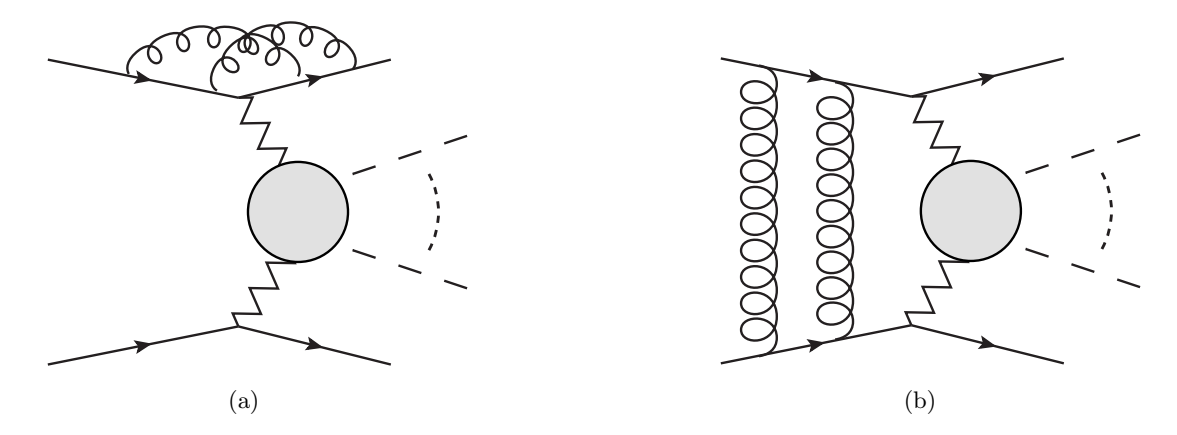


**Figure 2**: Representative diagrams for (a) factorizable and (b) non-factorizable NNLO-QCD corrections to VBF HH. The grey blob represents the  $VV \to HH$  sub-process. Figure reproduced from [24].

fully differential whereas the N<sup>3</sup>LO-QCD corrections are inclusive in the jet kinematics, but fully differential in the Higgs boson momenta. The code itself makes use of some general features of the POWHEG BOX, a modified implementation of the VBF H+3 jets process in the POWHEG BOX [36] and of the phase-space parameterization of the VBF HH process as implemented in VBFNLO [5]. The anomalous couplings have been implemented in v2.1.0 and can be obtained from https://github.com/alexanderkarlberg/proVBFH.

For the purpose of studying the sensitivity of the VBF HH process to Higgs couplings while fully taking QCD corrections into account, both proVBFHH and the inclusive standalone version of the proVBFHH program have been extended: The kappa framework has been implemented in such a way that values for the coupling modifiers  $\kappa_{\lambda}$ ,  $\kappa_{V}$ , and  $\kappa_{2V}$  can be set by the user. In proVBFHH the matrix element is expressed in terms of the DIS structure functions [37]. In this formalism the tensor related to the amplitude of the  $VV \to HH$  sub-process is expressed as [22, 38]

$$\mathcal{M}^{VVHH,\mu\nu} = 2\sqrt{2}G_{F}g^{\mu\nu} \left( \frac{2\kappa_{V}^{2}m_{V}^{4}}{(q_{1}+k_{1})^{2}-m_{V}^{2}+i\Gamma_{V}m_{V}} + \frac{2\kappa_{V}^{2}m_{V}^{4}}{(q_{1}+k_{2})^{2}-m_{V}^{2}+i\Gamma_{V}m_{V}} \right. \\ \left. + \frac{6v\kappa_{V}\kappa_{\lambda}m_{V}^{2}}{(k_{1}+k_{2})^{2}-m_{H}^{2}+i\Gamma_{H}m_{H}} + \kappa_{2V}m_{V}^{2} \right) \\ + \frac{\sqrt{2}G_{F}\kappa_{V}^{2}m_{V}^{4}}{(q_{1}+k_{1})^{2}-m_{V}^{2}} \frac{(2k_{1}^{\mu}+q_{1}^{\mu})(k_{2}^{\nu}-k_{1}^{\nu}-q_{1}^{\nu})}{m_{V}^{2}-i\Gamma_{V}m_{V}} \\ + \frac{\sqrt{2}G_{F}\kappa_{V}^{2}m_{V}^{4}}{(q_{1}+k_{2})^{2}-m_{V}^{2}} \frac{(2k_{2}^{\mu}+q_{1}^{\mu})(k_{1}^{\nu}-k_{2}^{\nu}-q_{1}^{\nu})}{m_{V}^{2}-i\Gamma_{V}m_{V}},$$

$$(2.2)$$

where  $k_1, k_2$  are the final state Higgs momenta,  $q_1$  and  $q_2$  are the vector boson momenta and momentum conservation yields  $k_1 + k_2 = q_1 + q_2$ . Here v is the vacuum expectation value of the Higgs field,  $G_F$  is Fermi's constant and  $\Gamma_V$  and  $m_V$  are the width and mass of the exchanged vector boson, respectively. The modified couplings are highlighted in colour.

When considering the QCD corrections to the diagrams shown in Fig. 1 they can

be divided into two separate contributions. The majority of the corrections come from diagrams where gluons only attach to a single quark line, cf. Fig 2a. These corrections are called *factorized* corrections, as they effectively factorize from the EW production. Starting at NNLO there are also corrections stemming from the exhange of two gluons between the two quark lines, cf. Fig. 2b. These *non-factorizable* corrections are colour-suppressed compared to their factorizable counterparts, but explicit studies of them in the eikonal approximation [24, 39–42] and beyond [43] have found that they receive a Glauber-phase enhancement. They are also sensitive to the exact details of the EW production, since the couplings of the Higgs bosons enter directly in the loops. In fact, in the Standard Model the non-factorizable corrections are somewhat suppressed by the unitarity cancellations between the different diagrams [24].

#### 2.2 Implementation in the POWHEG BOX

An implementation of the VBF HH process in the framework of the POWHEG BOX has not been available until now. We therefore developed such an implementation from scratch proceeding along similar lines as in the related VBS-induced VV + 2 jets processes [44–48].

In detail, the implementation of the VBF HH process required us to prepare matrix elements for all flavour combinations of external partons compatible with charge conservation at each interaction vertex at Born level, virtual and real-emission corrections, as well as colour- and spin correlated amplitudes for the computation of subtraction terms within the FKS-scheme [49] for the treatment of infrared divergences. To that end, we used the helicity-amplitude formalism of Ref. [50] for the computation of fermionic currents, amended by building blocks for bosonic tensors accounting for the  $VV \to HH$  subprocess within the SM and the kappa framework prepared with the help of a heavily customized version of the Madgraph 2 amplitude generator [51]. At Born level, only subprocesses of the type  $qq' \to qq'HH$  (where q and q' denote any light quark flavour) and crossing-related ones with external anti-quarks appear. The virtual contributions comprise gluonic loop corrections to either the upper or the lower quark line, resulting in a total expression proportional to the Born amplitude, similar to the case of VBF-induced single Higgs production discussed in [52], such that the finite part of the virtual corrections,  $\mathcal{V}_{\mathrm{fin}}$ , assumes the form

$$V_{\text{fin}} = C_F \left[ -\ln^2 \left( \frac{\mu_{\text{R}}^2}{q_1^2} \right) - 3\ln \left( \frac{\mu_{\text{R}}^2}{q_1^2} \right) - \ln^2 \left( \frac{\mu_{\text{R}}^2}{q_2^2} \right) - 3\ln \left( \frac{\mu_{\text{R}}^2}{q_2^2} \right) - 16 \right] \mathcal{B}, \tag{2.3}$$

As above,  $q_1$  and  $q_2$  denote the momenta of the two bosons exchanged in the t-channel,  $\mu_R$  is the renormalization scale,  $C_F = 4/3$ , and  $\mathcal{B}$  the Born amplitude.

For the real-emission contributions, matrix elements for all subprocesses with an additional external gluon g had to be developed. Similar to the Born case, for the computation of all subprocesses of the type  $qq' \rightarrow qq'gHH$  and crossing-related contributions we used the helicity-amplitude formalism of Ref. [50] supplemented by customized bosonic tensors for the  $VV \rightarrow HH$  sub-amplitudes. All matrix elements were implemented in such a way that, depending on the parameters chosen by the user in an editable input file, they can

account for the VBF HH production process in the SM, but also in the kappa framework with adjustable values of the couplings modifiers  $\kappa_{\lambda}$ ,  $\kappa_{2V}$ ,  $\kappa_{V}$ .

In addition to the partonic scattering amplitudes, the implementation of the VBF HH process in the POWHEG BOX V2 required us to provide a customized phase-parameterization. To that end, we adapted a respective routine of the provBFHH program to comply with the format requirements of the POWHEG BOX. Since the inclusive leading-order (LO) cross section for VBF HH is finite, no technical cuts are needed to obtain numerically stable results.

In order to validate our implementation, we have compared tree-level matrix elements for selected phase-space points with MadGraph-generated ones, finding full agreement. We have checked that the real-emission contributions approach their soft and collinear limits correctly. Results for a variety of kinematic distributions of all final-state particles at LO and NLO-QCD have been compared to those obtained with the proVBFHH program both within the SM and for non-unit values of the coupling modifiers. We found full agreement in each case.

# 3 Phenomenological results

In this section we present some representative phenomenological results using our new implementations.

### 3.1 Setup

POWHEG: pTdef = 1

We consider proton-proton collisions at the LHC with a centre-of-mass energy of  $\sqrt{s} = 13 \,\text{TeV}$ . For the parton shower results we use PYTHIA version 8.312 [31] with the Monash 2013 tune [53] and HERWIG7 version 7.3.0 [33]. We have adapted the matching procedure for HERWIG7 and PYTHIA from Ref. [54] and Ref. [55], i.e. we use the options

```
set/Herwig/Shower/ShowerHandler: MaxPtIsMuFYes
set/Herwig/Shower/ShowerHandler: RestrictPhasespaceYes
in HERWIG7 and the settings

POWHEG: veto = 1
POWHEG: pThard = 0
POWHEG: pTemt = 0
POWHEG: emitted = 0
```

in the context of the PowhegHooks class contained in PYTHIA.

Both the dipole-local PYTHIA shower [56] and the Vincia antenna shower [32] are considered. As has been noted in the past the default PYTHIA shower should be avoided, in particular for VBF processes, as it breaks coherence which leads to an excess of central jet activity [34, 35, 57]. Underlying event (UE), hadronization, multi-parton interactions (MPI), and QED radiation effects are turned off.

For the parton distribution functions (PDFs) of the protons we use the PDF set NNPDF40MC\_nnlo\_as\_01180 [58] as obtained from the LHAPDF6 repository [59] with the associated strong coupling  $\alpha_s(m_Z) = 0.118$ . The number of active quark flavours is set to five. For the values of the masses and widths of the W, Z and H bosons we use [60]:

$$m_W = 80.3692 \,\text{GeV}, \qquad \Gamma_W = 2.085 \,\text{GeV},$$
 (3.1)

$$m_Z = 91.1880 \,\text{GeV}, \qquad \Gamma_Z = 2.4955 \,\text{GeV},$$
 (3.2)

$$m_H = 125.2 \,\text{GeV}, \qquad \Gamma_H = 3.7 \times 10^{-3} \,\text{GeV}.$$
 (3.3)

We apply the  $G_{\mu}$  scheme [61], where  $\alpha$  and the weak mixing angle are calculated from the Fermi constant  $G_{\mu} = 1.16637 \times 10^{-5} \text{ GeV}^{-2}$ ,  $m_W$  and  $m_Z$  via tree-level EW relations. For the Cabibbo-Kobayashi-Maskawa matrix a diagonal form is assumed and we apply the Bornzerodamp mechanism as already implemented in the POWHEG BOX, to dynamically separate the real emission matrix element into its singular and non-singular part. Since the negative-weight fraction is not negligible (about 20% in a standard run), we also make use of folding [62] to reduce the fraction to a few percent.

The factorization and renormalization scales,  $\mu_R = \xi_R \mu_0$  and  $\mu_F = \xi_F \mu_0$ , are set according to

$$\mu_0^2 = \frac{m_H}{2} \sqrt{\left(\frac{m_H}{2}\right)^2 + p_{T,HH}^2}, \tag{3.4}$$

where  $p_{T,HH}$  denotes the transverse momentum of the Higgs-pair system. Scale uncertainties are estimated by a 7-point variation of the scale factors  $\xi_{\rm R}$  and  $\xi_{\rm F}$  by factors between 0.5 and 2

For our numerical studies we reconstruct jets according to the anti- $k_T$  algorithm [63] with a distance parameter of R = 0.4 using the FastJet package [64], version 3.3.4. We require at least two hard jets j with transverse momenta and rapidities in the range

$$p_{T,j} > 25 \,\text{GeV}, \qquad |y_j| < 4.5,$$
 (3.5)

The two hardest jets fulfilling this criterion are referred to as tagging jets. The two tagging jets are required to exhibit a large invariant mass and rapidity separation,

$$m_{jj}^{\rm tag} > 600\,{\rm GeV}\,, \qquad \Delta y_{jj}^{\rm tag} = |y_{j_1}^{\rm tag} - y_{j_2}^{\rm tag}| > 4.5, \qquad y_{j_1}^{\rm tag} \cdot y_{j_2}^{\rm tag} < 0. \eqno(3.6)$$

Whenever we consider subleading jets, we apply additional cuts to make these jets well-identifiable. For instance, for some distributions of the third-hardest jet, to be discussed below, in addition to the cuts of Eqs. (3.5)–(3.6), we require

$$p_{T,j_3} > 25 \,\text{GeV}, \qquad |y_{j_3}| < 4.5.$$
 (3.7)

No cuts are applied to the Higgs bosons.

The results for the fiducial cross section after cuts at different accuracy are shown in Tab. 1.

accuracy	$\sigma$ [fb]	ratio to NLO
LO	0.668	1.087
NLO	0.614	1
NNLO	0.603	0.982
NLO+PYTHIA8	$0.585^{+0.007}_{-0.009}$	0.953
$\mathrm{NLO}+\mathtt{Vincia}$	$0.592^{+0.007}_{-0.010}$	0.964
${ m NLO}{+}{ m HERWIG7}$	$0.575^{+0.013}_{-0.007}$	0.936

**Table 1:** SM fiducial cross sections in fb after the cuts of Eqs. (3.5)–(3.6) at different accuracies and ratio to NLO. Statistical errors are beyond the quoted precision. Scale uncertainties are indicated by the subscript and superscript for NLO+PS accuracy only.

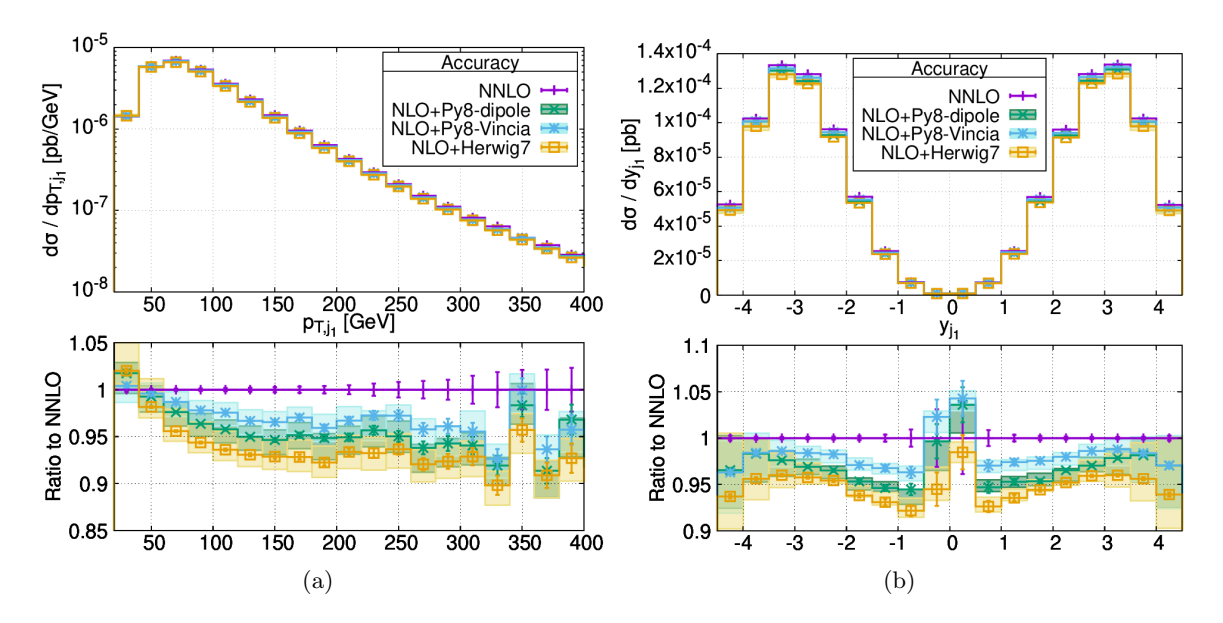
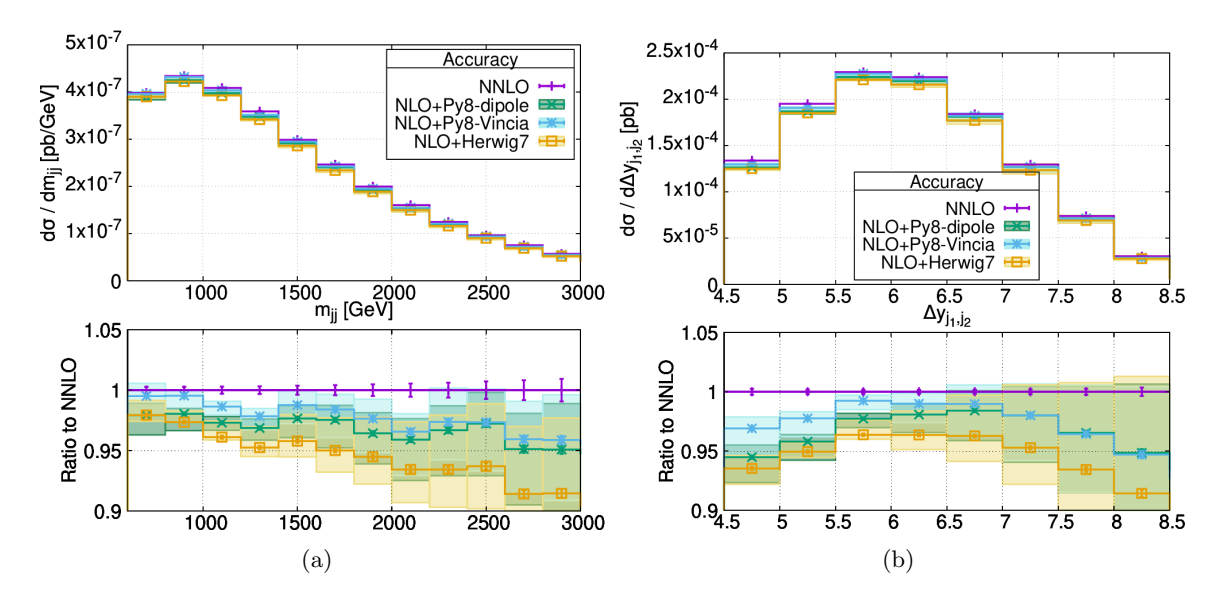


Figure 3: Transverse-momentum (left) and rapidity distributions (right) of the hardest tagging jet for the VBF HH process as described in the text within the cuts of Eqs. (3.5)–(3.6) at NNLO (magenta), NLO+PS using HERWIG7 (orange) or PYTHIA8 with the dipole shower (green) and the Vincia shower (blue), and their ratios to the respective NNLO results (lower panels). Error bars indicate statistical uncertainties, bands correspond to a 7-point variation around the central scale  $\mu_0$  of each curve.

#### 3.2 Parton-shower matched results

Let us first consider VBF HH production in the framework of the SM. In Fig. 3 the transverse-momentum and rapidity distributions of the hardest tagging jet are shown for the NNLO and the NLO+PS predictions using either HERWIG7 or PYTHIA8, for the latter using either the "dipole" shower or the Vincia shower. We find relatively good agreement between all predictions with a slight redistribution of events from high to low values of



**Figure 4**: Similar to Fig. 3, but for the invariant mass distribution (left) and the rapidity separation (right) of the two tagging jets.

transverse momentum in the NLO+PS results as compared to the NNLO predictions, and a moderate change of shape in the rapidity distributions, with the NLO+PS results tending to more central values. The different shower options yield similar results, with the Vincia shower being closest to the NNLO benchmark results and the HERWIG7 shower being furthest away from the NNLO values. However, the differences between the various showers are mostly contained in the normalization, with very similar shapes across the three variants.

A similar tendency can be observed in invariant mass distribution and rapidity separation of the two tagging jets, shown in Fig. 4. For these distributions the NLO+PS predictions are consistently below the fixed-order predictions. In particular, at large values of  $m_{jj}^{\rm tag}$  the extra radiation emerging because of the PS results in a slight shift of the taggings jets' kinematics, resulting in fewer events passing the selection cuts. This feature is rather genuine and does not change if instead of HERWIG either of the PYTHIA8 shower options is used.

In Fig. 5 the transverse momentum distributions of the hardest Higgs boson and the Higgs-pair system are shown. These exhibit a similar trend as the distributions of the transverse momentum of the hardest tagging jet and of the invariant mass of the tagging jet system with the NLO+PS predictions lying a few percent below the fixed-order NNLO predictions.

In Fig. 6 the transverse-momentum and relative rapidity of the third jet with respect to the tagging-jet system are considered. The latter is defined as

$$y_{j_3}^{\star} = y_{j_3} - \frac{y_{j_1} + y_{j_2}}{2} \,. \tag{3.8}$$

We note that a third jet only enters via the real-emission contributions in the NLO cal-

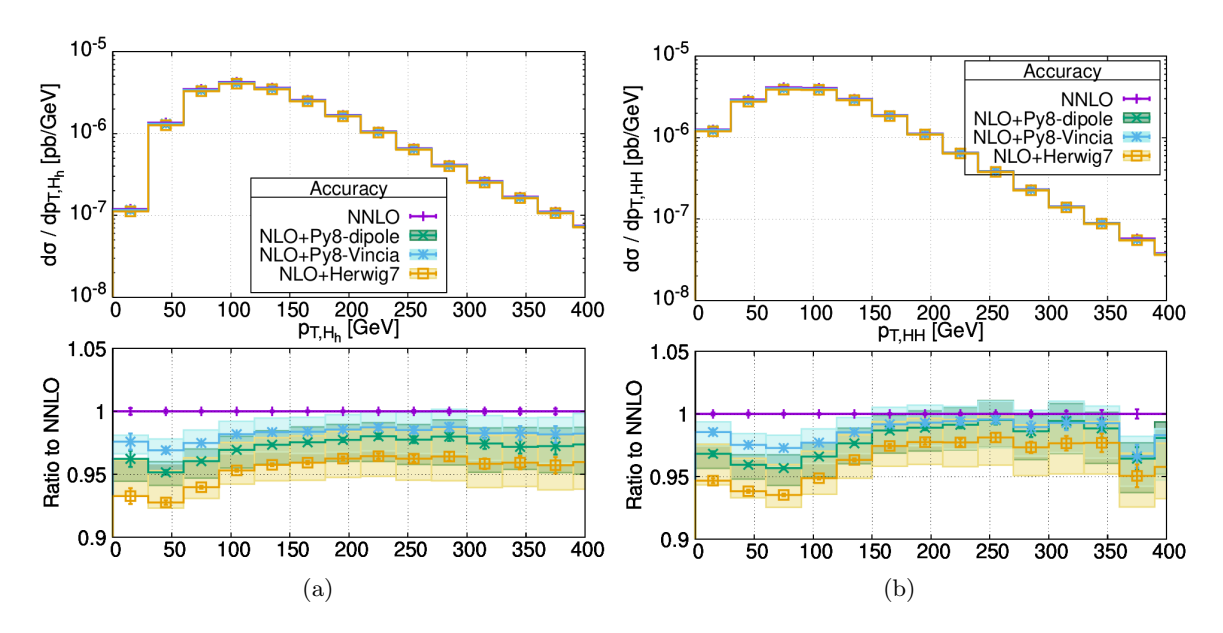


**Figure 5**: Similar to Fig. 3, but for the transverse momentum distribution of the hardest Higgs boson (left) and of the Higgs-pair system (right).

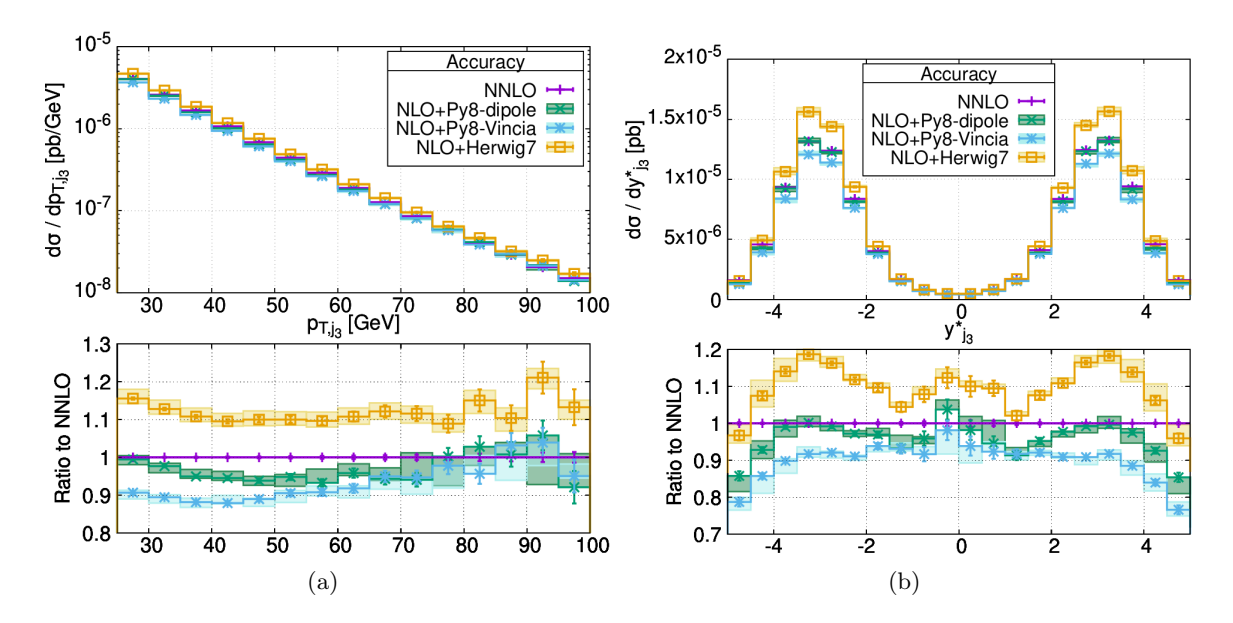


**Figure 6**: Similar to Fig. 3, but for the transverse-momentum and the relative rapidity distribution of the third jet as defined in Eq. (3.8). The additional cuts of Eq. (3.7) are applied.

culation of the VBF HH process, and it thus only accounted for with tree-level accuracy in our NLO results. NLO accuracy for distributions of the third jet is achieved by the NNLO calculation of the HH+2 jets process. In the NLO+PS predictions, a third jet can also result from PS emissions. As apparent from Fig. 6, the NLO+PS prediction using the

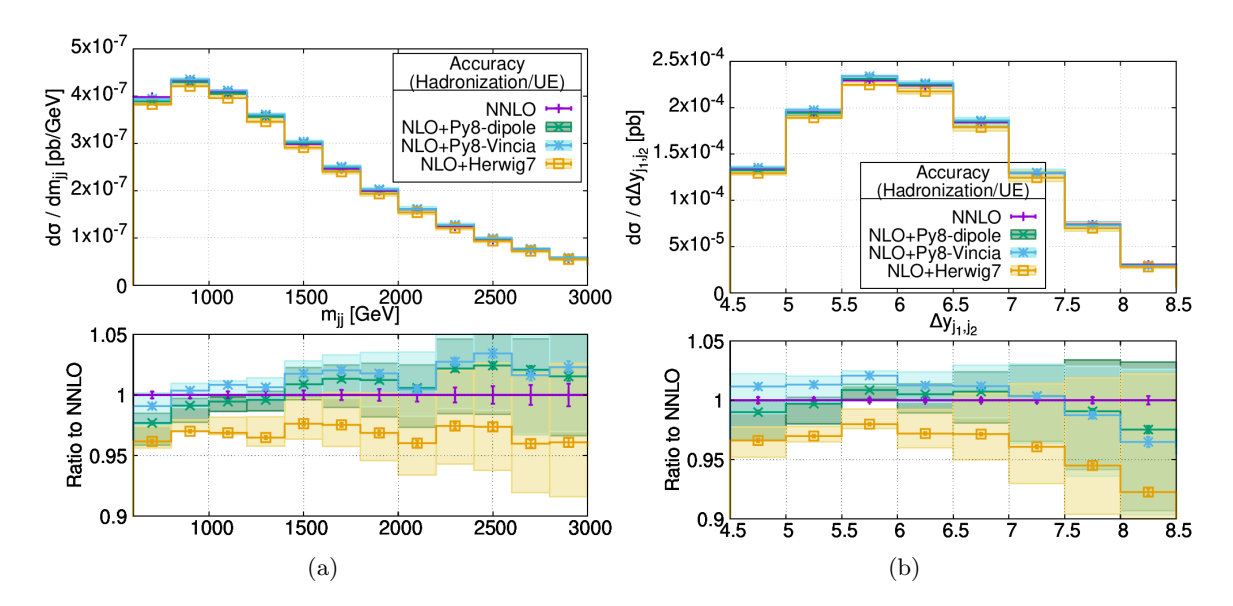


Figure 7: Similar to Fig. 4, but with underlying event and hadronization turned on.

dipole version of PYTHIA8 provides a decent approximation of the NNLO results, whereas Vincia sits somewhat below. The HERWIG7 predictions, on the other hand, overshoot the PYTHIA8 results by 10 to 20%. The larger spread in predictions is expected due to the lower perturbative accuracy for the third jet, but should be taken into account whenever the third jet enters an experimental analysis. In order to reduce this uncertainty, the third jet would have to be matched at NLO, as was done in single Higgs VBF production [36].

### 3.3 Hadronization and underlying event

To further study the impact of parton shower settings on the observables we also display the results with hadronization and underlying event turned on in the parton shower in Fig. 7 for the invariant mass distribution and the rapidity separation of the two tagging jets, and in Fig. 8 for the transverse momentum and the relative rapidity distribution of the third jet.

We observe that for observables concerning the tagging jets the hadronization/UE only has a small impact increasing the ratio to NNLO by a few percent while keeping the relative spread of the NLO+PS predictions mostly unchanged. The impact on the third jet observables is much larger filling the central region between the two tagging jets as apparent from Fig. 8 (right). This effect has been observed in the past for other VBF processes [65].

#### 3.4 Impact of anomalous couplings

With these features of the perturbative corrections for the SM predictions in mind, let us now turn towards an analysis of anomalous Higgs couplings using the kappa framework introduced in Sec. 2. Since the NLO+PS predictions have been found to provide a good approximation of the full NNLO results, in the following we will only show results obtained with our POWHEG BOX implementation using the Vincia shower [32] of PYTHIA8.

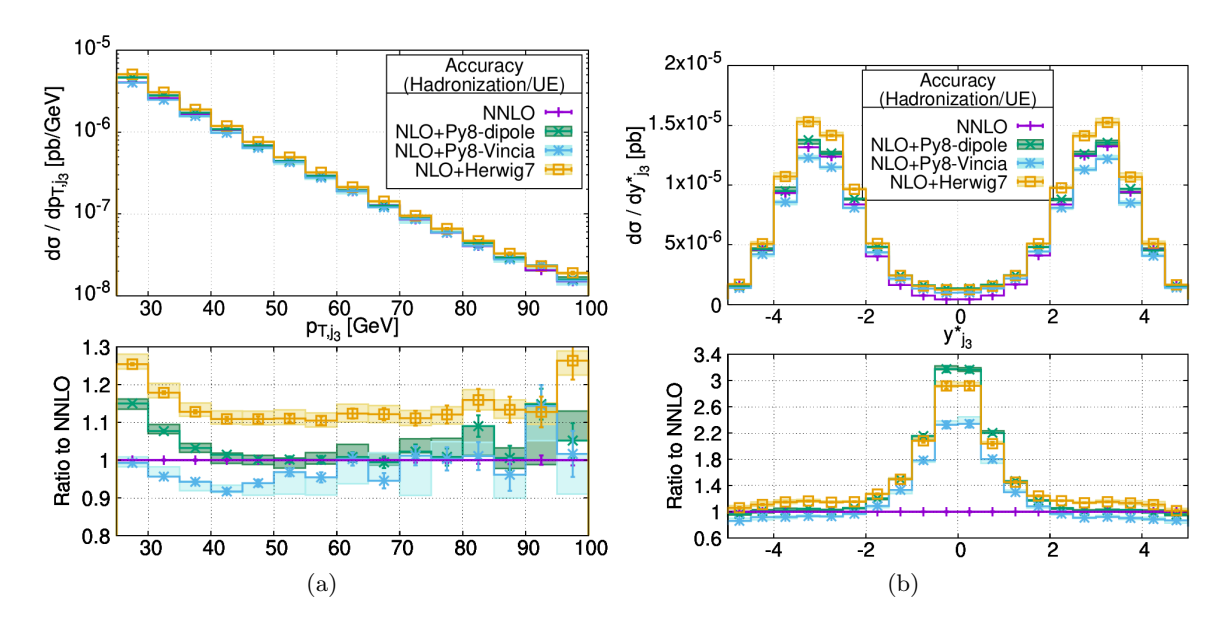


Figure 8: Similar to Fig. 6, but with underlying event and hadronization turned on.

We consider values of the coupling factors compatible with experimental bounds, i.e.  $0.6 < \kappa_{2V} < 1.5$  [3],  $0.98 < \kappa_{V} < 1.1$  [66] (we have extracted the  $2\sigma$  limit from Fig. 6),  $-1.2 < \kappa_{\lambda} < 7.2$  [3].

In Tab. 2 we display the fiducial cross section results after VBF cuts for different values of the anomalous couplings and the ratio to the SM values at NLO+PS, using the Vincia shower prediction.

In Fig. 9 the transverse-momentum distributions of the hardest Higgs boson and of the Higgs-pair system are considered within the SM, and for selected scenarios with one coupling modifier being set to a non-SM value compatible with experimental bounds while all other couplings retain their SM value. When the coupling modifiers are set to values

Coupling factor	$\sigma$ [fb]	ratio to SM
SM	0.592	1
$\kappa_{2V} = 1.5$	1.14	1.93
$\kappa_{2V} = 0.6$	2.57	4.34
$\kappa_V = 1.1$	1.86	3.15
$\kappa_V = 0.98$	0.463	0.781
$\kappa_{\lambda} = 7.2$	13.0	21.9
$\kappa_{\lambda} = -1.2$	3.71	6.27

**Table 2**: Fiducial cross sections in fb after the cuts of Eqs. (3.5)–(3.6) for the different anomalous couplings and the ratio to the SM value for NLO+Vincia. Statistical errors are beyond the quoted precision.

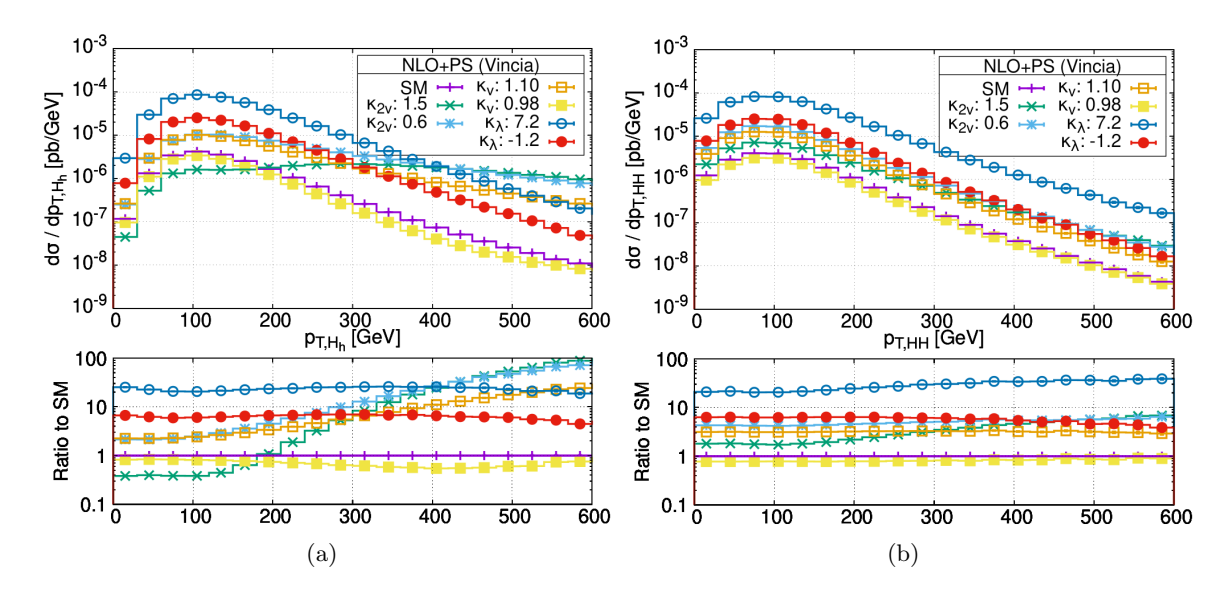


Figure 9: Transverse-momentum distribution of the hardest Higgs boson (left) and of the Higgs-pair system (right) for the VBF HH process as described in the text within the cuts of Eqs. (3.5)–(3.6) at NLO+PS accuracy within the SM (magenta), and for different values of the Higgs coupling modifiers  $\kappa_i$  as indicated in the legend, together with their ratios to the respective SM results. Statistical uncertainties are indicated by error bars (but mostly too small to be visible).

significantly different from 1, both of the considered distributions change their normalization and shape considerably. This is due to the very delicate unitarity cancellations which are present in the Higgs sector. The large sensitivity to these couplings highlights the importance of the VBF HH process in the Higgs program. It is clear that for such large deviations of the couplings from their SM values the validity of the approach breaks down. More refined models would be needed to understand the very mechanism resulting in a genuinely non-SM type behavior of the relevant Higgs couplings. Indeed, the kappa framework must be applied only to *identify* deviations from the SM expectation, but cannot be expected to provide a deeper understanding of the origin of such deviations. For instance, the so-called K-matrix unitarisation scheme to regulate the high-energy behavior of VBF and vector boson scattering processes in the presence of physics beyond the SM has been explored in [67]. We believe that nonetheless it is useful to provide tools capable to compute predictions in a framework that is used by many experimental analyses to simplify the comparison of data with theoretical predictions.

Finally, we note that the interplay between the anomalous couplings and the NLO-QCD corrections are expected to be very mild, as the corrections completely factorize from the EW production of the two Higgs bosons. We have verified that the NLO corrections to the fiducial cross section in this setup vary by less than a percent. This can also be observed for the total inclusive cross section in figures 8 and 9 in Ref. [22].

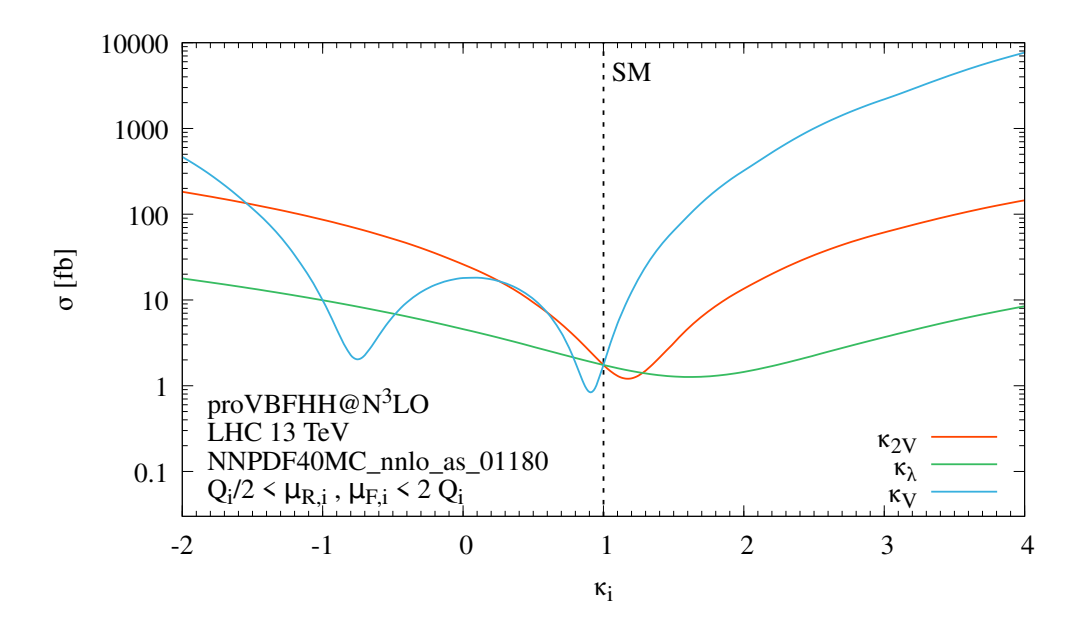


Figure 10: The inclusive VBF HH cross section in fb as a function of  $\kappa_{2V}$  (red),  $\kappa_{\lambda}$  (green), and  $\kappa_{V}$  (blue) using provBFHH at N<sup>3</sup>LO. The SM value is indicated with a dashed line. The QCD scale uncertainty is entirely contained within the line width of the plot.

#### 3.4.1 Inclusive results at N<sup>3</sup>LO

Our discussion so far has been focused on the new POWHEG BOX implementation. As mentioned already in the introduction we have also implemented the anomalous couplings in the proVBFHH program. That implementation served as a cross check of the POWHEG BOX implementation, but can in particular also be used to provide high accuracy predictions for quantities inclusive in the jet kinematics, such as the inclusive cross section and Higgs boson transverse momentum.

To showcase this, in Fig. 10 we show a scan of the three coupling modifiers  $\kappa_{2V}$ ,  $\kappa_{\lambda}$ , and  $\kappa_{V}$  in the range [-2:4] in the same setup as above at N³LO, but without any cuts imposed. The renormalization and factorization scales are chosen separately for each quark line, as the momentum squared of the vector boson attached to that quark,  $-q_{i}^{2}$ . The scales are varied by a factor two up and down, yielding a variation in the permille range, which is completely contained within the line width in the plot. The figure clearly shows the very strong dependence of the cross section on the coupling modifiers. From this plot it is also clear that one cannot fully distinguish the three couplings from an inclusive measurement alone, but rather that one needs to complement the inclusive information with distributions obtained with for instance our new POWHEG BOX implementation. In fact, there must exist a hypersurface in the  $\{\kappa_{2V}, \kappa_{\lambda}, \kappa_{V}\}$ -space where the inclusive cross section is identical to the SM value, making an inclusive measurement in that case useless. One advantage, however, of the proVBFHH code, beyond its state-of-the-art perturbative accuracy, is that it is extremely fast, and that plots like the above scan can in principle be obtained on a laptop.

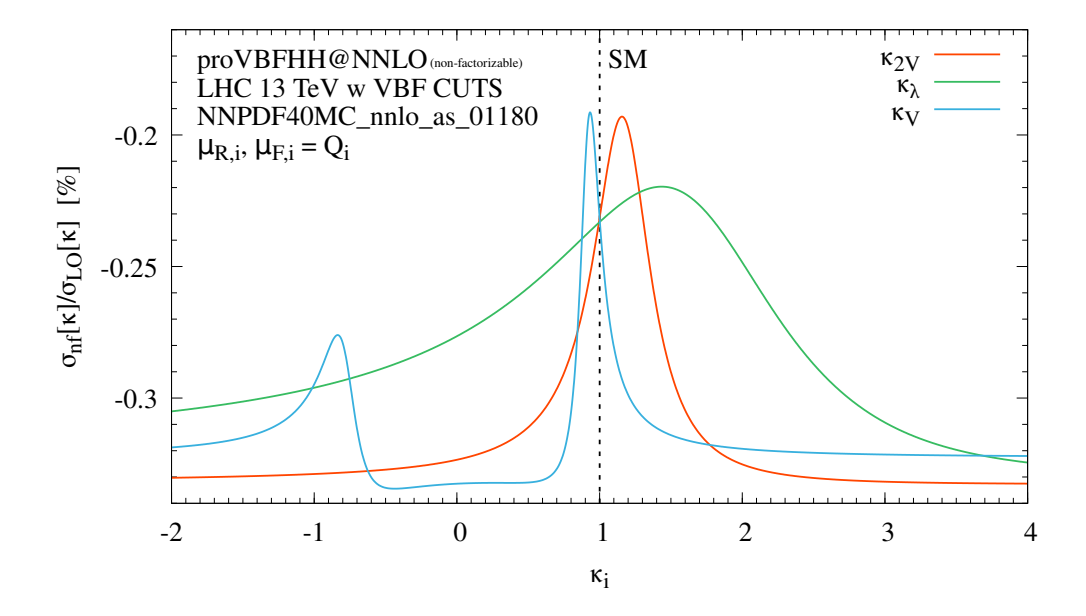


Figure 11: The relative impact of non-factorizable NNLO corrections to the VBF HH process in percent as a function of  $\kappa_{2V}$  (red),  $\kappa_{\lambda}$  (green), and  $\kappa_{V}$  (blue) obtained with proVBFHH. The SM value is indicated with a dashed line. The cross section is computed within the VBF cuts of Eqs. (3.5)–(3.6).

We note that the more complicated dependence on  $\kappa_V$  compared to the two other coupling modifiers comes down to the fact that this coupling enters quadratically in Eq. (2.2) as opposed to linearly. At the level of the cross section this means that the coupling enters quartically as opposed to quadratically. As stated already above, the factorized QCD corrections are almost constant with respect to the anomalous couplings.

## 3.4.2 Impact on non-factorizable corrections

Unlike the factorizable corrections discussed above the non-factorizable corrections are very sensitive to the anomalous couplings. This can be understood by realising that the anomalous couplings spoil the delicate unitarity cancellation taking place in the  $VV \to HH$  sub-process. Since the non-factorizable corrections act slightly differently on each of the sub-processes, and since they are somewhat suppressed in the SM due to this unitarity cancellation, they can be enhanced significantly in the presence of anomalous couplings.

In Fig. 11 we show this effect under the VBF cuts of Eqs. (3.5)–(3.6).<sup>1</sup> In the SM, under these cuts, the relative contribution of the NNLO non-factorizable corrections is -0.23% (to be compared to the factorizable NLO $\rightarrow$ NNLO correction of -1.7%). From Fig. 11 we see that this can grow by more than 40% to -0.33%. Phenomenologically this has very little impact, since the corrections are still sub-leading, but it is of some theoretical

<sup>&</sup>lt;sup>1</sup>Here we apply VBF cuts because the NNLO non-factorizable corrections are computed in the eikonal approximation which is only strictly valid when  $m_{jj}^{\text{tag}} \gg p_{T,j_i}$ ,  $p_{T,H_i}$ .

interest. Typically, the VBF approximation is justified by the statement that contributions beyond the factorized approximation in a strict sense are small.

If non-factorizable corrections change when anomalous couplings are considered this may have an impact of the quality of the VBF approximation. We note that in the recent work of Ref. [68] the authors considered EW HH+2 jets production retaining all relevant diagrams, including non-factorizable corrections that appear in the s-channel. In figure 3 of that reference they report that the NLO QCD corrections are not entirely flat. We suspect that this is due to the non-factorizable corrections, and would indicate that the quality of the VBF approximation deteriorates when anomalous couplings are considered. We leave a detailed study of this effect for the future.

## 4 Conclusions and outlook

In this article we presented an extension of the provBFHH tool to account for non-SM values of the Higgs couplings  $g_{HHH}$ ,  $g_{HHVV}$ , and  $g_{HVV}$  in the kappa framework. Moreover, we developed a new implementation of the VBF-induced HH+2 jets process in the POWHEG BOX. With this tool fully differential NLO predictions matched to PS programs such as PYTHIA or HERWIG can be obtained both within the SM and the kappa framework. We note that this is the first time that NLO+PS accurate predictions can be obtained with PYTHIA. Having access to NLO-accurate differential distributions is important to disentangle the effect of the three anomalous couplings, highlighting the need to have them implemented in a flexible tool like the one presented here.

Using these tools we systematically explored the impact of perturbative corrections and parton shower effects for the SM and found that the NLO+PS results provide a good approximation of the NNLO predictions for distributions of the tagging jets and Higgs bosons. Larger differences are found for observables related to subleading jets. We then investigated the sensitivity of selected observables on various Higgs coupling factors and found that non-SM values compatible with current experimental bounds can result in distributions differing dramatically from the corresponding SM expectations.

Finally we also studied the impact of anomalous couplings when considering non-factorizable corrections to VBF HH. We found that they are highly sensitive to the exact coupling values, and can be enhanced by as much as 40% compared to in the SM.

It is worth keeping in mind that our analysis does not take into account any EW corrections. Since the effect of EW corrections is most pronounced in tails of distributions, where the effect of anomalous couplings also tend to show up, it might be important to study their interplay. We leave that to future studies.

The latest version of the provBFHH tool can be obtained from https://github.com/alexanderkarlberg/provBFH. The new NLO+PS code is made available via the POWHEG BOX V2 repository, see https://powhegbox.mib.infn.it/.

# Note added

While finalising this work we were made aware of Ref. [68]. Our work and that reference are somewhat complementary, as we have focused on a parton shower matched implementation of EW Higgs pair production in the VBF approximation, and compared it to an NNLO computation, whereas Ref. [68] is at fixed order but goes beyond the structure-function approach. We leave a detailed comparison of our implementations for future work.

# Acknowledgements

We are grateful to Gudrun Heinrich, Jens Braun, Marius Höfer, and Pia Bredt for sharing their draft with us before publication. BJ and SR acknowledge support by the state of Baden-Württemberg through bwHPC and the German Research Foundation (DFG) through grant no INST 39/963-1 FUGG.

## References

- [1] ATLAS collaboration, G. Aad et al., Observation of a new particle in the search for the Standard Model Higgs boson with the ATLAS detector at the LHC, Phys. Lett. B 716 (2012) 1 [1207.7214].
- [2] CMS collaboration, S. Chatrchyan et al., Observation of a New Boson at a Mass of 125 GeV with the CMS Experiment at the LHC, Phys. Lett. B 716 (2012) 30 [1207.7235].
- [3] ATLAS collaboration, G. Aad et al., Combination of Searches for Higgs Boson Pair Production in pp Collisions at s=13 TeV with the ATLAS Detector, Phys. Rev. Lett. 133 (2024) 101801 [2406.09971].
- [4] CMS collaboration, Combination of searches for nonresonant Higgs boson pair production in proton-proton collisions at sqrt(s) = 13 TeV, 2024.
- [5] J. Baglio, A. Djouadi, R. Gröber, M. M. Mühlleitner, J. Quevillon and M. Spira, The measurement of the Higgs self-coupling at the LHC: theoretical status, JHEP 04 (2013) 151 [1212.5581].
- [6] F. Bishara, R. Contino and J. Rojo, Higgs pair production in vector-boson fusion at the LHC and beyond, Eur. Phys. J. C 77 (2017) 481 [1611.03860].
- [7] F. Boudjema and A. Semenov, Measurements of the SUSY Higgs selfcouplings and the reconstruction of the Higgs potential, Phys. Rev. D 66 (2002) 095007 [hep-ph/0201219].
- [8] M. Moretti, S. Moretti, F. Piccinini, R. Pittau and A. D. Polosa, Beyond the standard model Higgs boson self-couplings at the LHC, in 32nd International Conference on High Energy Physics, pp. 1256–1259, 11, 2004, hep-ph/0411039, DOI.
- [9] M. Moretti, S. Moretti, F. Piccinini, R. Pittau and A. D. Polosa, *Higgs boson self-couplings* at the LHC as a probe of extended Higgs sectors, *JHEP* **02** (2005) 024 [hep-ph/0410334].
- [10] M. J. Dolan, C. Englert, N. Greiner and M. Spannowsky, Further on up the road: hhjj production at the LHC, Phys. Rev. Lett. 112 (2014) 101802 [1310.1084].
- [11] M. J. Dolan, C. Englert, N. Greiner, K. Nordstrom and M. Spannowsky, hhjj production at the LHC, Eur. Phys. J. C 75 (2015) 387 [1506.08008].

- [12] K. Arnold et al., VBFNLO: A Parton level Monte Carlo for processes with electroweak bosons, Comput. Phys. Commun. 180 (2009) 1661 [0811.4559].
- [13] J. Baglio et al., VBFNLO: A parton level Monte Carlo for processes with electroweak bosons
   Manual for Version 3.0, 1107.4038.
- [14] J. Baglio et al., Release note: VBFNLO 3.0, Eur. Phys. J. C 84 (2024) 1003 [2405.06990].
- [15] T. Figy, Next-to-leading order QCD corrections to light Higgs Pair production via vector boson fusion, Mod. Phys. Lett. A 23 (2008) 1961 [0806.2200].
- [16] Anisha, D. Domenech, C. Englert, M. J. Herrero and R. A. Morales, HEFT's appraisal of triple (versus double) Higgs weak boson fusion, Phys. Rev. D 111 (2025) 055004 [2407.20706].
- [17] J. Alwall, R. Frederix, S. Frixione, V. Hirschi, F. Maltoni, O. Mattelaer et al., The automated computation of tree-level and next-to-leading order differential cross sections, and their matching to parton shower simulations, JHEP 07 (2014) 079 [1405.0301].
- [18] R. Frederix, S. Frixione, V. Hirschi, F. Maltoni, O. Mattelaer, P. Torrielli et al., Higgs pair production at the LHC with NLO and parton-shower effects, Phys. Lett. B 732 (2014) 142 [1401.7340].
- [19] L.-S. Ling, R.-Y. Zhang, W.-G. Ma, L. Guo, W.-H. Li and X.-Z. Li, NNLO QCD corrections to Higgs pair production via vector boson fusion at hadron colliders, Phys. Rev. D 89 (2014) 073001 [1401.7754].
- [20] M. Cacciari, F. A. Dreyer, A. Karlberg, G. P. Salam and G. Zanderighi, Fully Differential Vector-Boson-Fusion Higgs Production at Next-to-Next-to-Leading Order, Phys. Rev. Lett. 115 (2015) 082002 [1506.02660].
- [21] F. A. Dreyer and A. Karlberg, Fully differential Vector-Boson Fusion Higgs Pair Production at Next-to-Next-to-Leading Order, Phys. Rev. D 99 (2019) 074028 [1811.07918].
- [22] F. A. Dreyer and A. Karlberg, Vector-Boson Fusion Higgs Pair Production at N<sup>3</sup>LO, Phys. Rev. D 98 (2018) 114016 [1811.07906].
- [23] F. A. Dreyer, A. Karlberg, J.-N. Lang and M. Pellen, Precise predictions for double-Higgs production via vector-boson fusion, Eur. Phys. J. C 80 (2020) 1037 [2005.13341].
- [24] F. A. Dreyer, A. Karlberg and L. Tancredi, On the impact of non-factorisable corrections in VBF single and double Higgs production, JHEP 10 (2020) 131 [2005.11334].
- [25] F. A. Dreyer and A. Karlberg, Vector-Boson Fusion Higgs Production at Three Loops in QCD, Phys. Rev. Lett. 117 (2016) 072001 [1606.00840].
- [26] S. Alioli, P. Nason, C. Oleari and E. Re, A general framework for implementing NLO calculations in shower Monte Carlo programs: the POWHEG BOX, JHEP 06 (2010) 043 [1002.2581].
- [27] P. Nason, A New method for combining NLO QCD with shower Monte Carlo algorithms, JHEP 11 (2004) 040 [hep-ph/0409146].
- [28] S. Frixione, P. Nason and C. Oleari, Matching NLO QCD computations with Parton Shower simulations: the POWHEG method, JHEP 11 (2007) 070 [0709.2092].
- [29] K. Hagiwara, S. Ishihara, R. Szalapski and D. Zeppenfeld, Low-energy effects of new interactions in the electroweak boson sector, Phys. Rev. D 48 (1993) 2182.

- [30] LHC HIGGS CROSS SECTION WORKING GROUP collaboration, A. David, A. Denner, M. Duehrssen, M. Grazzini, C. Grojean, G. Passarino et al., LHC HXSWG interim recommendations to explore the coupling structure of a Higgs-like particle, 1209.0040.
- [31] C. Bierlich et al., A comprehensive guide to the physics and usage of PYTHIA 8.3, SciPost Phys. Codeb. 2022 (2022) 8 [2203.11601].
- [32] N. Fischer, S. Prestel, M. Ritzmann and P. Skands, Vincia for Hadron Colliders, Eur. Phys. J. C 76 (2016) 589 [1605.06142].
- [33] G. Bewick et al., Herwig 7.3 release note, Eur. Phys. J. C 84 (2024) 1053 [2312.05175].
- [34] A. Ballestrero et al., Precise predictions for same-sign W-boson scattering at the LHC, Eur. Phys. J. C 78 (2018) 671 [1803.07943].
- [35] B. Jäger, A. Karlberg, S. Plätzer, J. Scheller and M. Zaro, *Parton-shower effects in Higgs production via Vector-Boson Fusion*, *Eur. Phys. J. C* **80** (2020) 756 [2003.12435].
- [36] B. Jäger, F. Schissler and D. Zeppenfeld, Parton-shower effects on Higgs boson production via vector-boson fusion in association with three jets, JHEP 07 (2014) 125 [1405.6950].
- [37] T. Han, G. Valencia and S. Willenbrock, Structure function approach to vector boson scattering in p p collisions, Phys. Rev. Lett. 69 (1992) 3274 [hep-ph/9206246].
- [38] A. Dobrovolskaya and V. Novikov, On heavy Higgs boson production, Z. Phys. C 52 (1991) 427.
- [39] T. Liu, K. Melnikov and A. A. Penin, Nonfactorizable QCD Effects in Higgs Boson Production via Vector Boson Fusion, Phys. Rev. Lett. 123 (2019) 122002 [1906.10899].
- [40] L. Gates, On Evaluation of Nonfactorizable Corrections to Higgs Boson Production via Vector Boson Fusion, Phys. Lett. B 846 (2023) 138191 [2305.04407].
- [41] K. Asteriadis, C. Brønnum-Hansen and K. Melnikov, Nonfactorizable corrections to Higgs boson production in weak boson fusion, Phys. Rev. D 109 (2024) 014031 [2305.08016].
- [42] C. Brønnum-Hansen, M.-M. Long and K. Melnikov, Scale dependence of non-factorizable virtual corrections to Higgs boson production in weak boson fusion, JHEP 11 (2023) 130 [2309.06292].
- [43] M.-M. Long, K. Melnikov and J. Quarroz, Non-factorizable virtual corrections to Higgs boson production in weak boson fusion beyond the eikonal approximation, JHEP 07 (2023) 035 [2305.12937].
- [44] B. Jager and G. Zanderighi, NLO corrections to electroweak and QCD production of W+W+ plus two jets in the POWHEGBOX, JHEP 11 (2011) 055 [1108.0864].
- [45] B. Jager and G. Zanderighi, Electroweak W+W-jj prodution at NLO in QCD matched with parton shower in the POWHEG-BOX, JHEP 04 (2013) 024 [1301.1695].
- [46] B. Jäger, A. Karlberg and G. Zanderighi, Electroweak ZZjj production in the Standard Model and beyond in the POWHEG-BOX V2, JHEP 03 (2014) 141 [1312.3252].
- [47] B. Jager, A. Karlberg and J. Scheller, Parton-shower effects in electroweak WZjj production at the next-to-leading order of QCD, Eur. Phys. J. C 79 (2019) 226 [1812.05118].
- [48] B. Jäger, A. Karlberg and S. Reinhardt, QCD effects in electroweak WZjj production at current and future hadron colliders, Eur. Phys. J. C 84 (2024) 587 [2403.12192].

- [49] S. Frixione, Z. Kunszt and A. Signer, Three jet cross-sections to next-to-leading order, Nucl. Phys. B 467 (1996) 399 [hep-ph/9512328].
- [50] K. Hagiwara and D. Zeppenfeld, Amplitudes for Multiparton Processes Involving a Current at e+ e-, e+- p, and Hadron Colliders, Nucl. Phys. B 313 (1989) 560.
- [51] T. Stelzer and W. F. Long, Automatic generation of tree level helicity amplitudes, Comput. Phys. Commun. 81 (1994) 357 [hep-ph/9401258].
- [52] P. Nason and C. Oleari, NLO Higgs boson production via vector-boson fusion matched with shower in POWHEG, JHEP 02 (2010) 037 [0911.5299].
- [53] P. Skands, S. Carrazza and J. Rojo, Tuning PYTHIA 8.1: the Monash 2013 Tune, Eur. Phys. J. C 74 (2014) 3024 [1404.5630].
- [54] S. Ferrario Ravasio and C. Oleari, NLO + parton-shower generator for **W**c production in the POWHEG BOX RES, Eur. Phys. J. C 83 (2023) 684 [2304.13791].
- [55] A. Banfi, S. Ferrario Ravasio, B. Jäger, A. Karlberg, F. Reichenbach and G. Zanderighi, A POWHEG generator for deep inelastic scattering, JHEP 02 (2024) 023 [2309.02127].
- [56] B. Cabouat and T. Sjöstrand, Some Dipole Shower Studies, Eur. Phys. J. C 78 (2018) 226 [1710.00391].
- [57] S. Höche, S. Mrenna, S. Payne, C. T. Preuss and P. Skands, A Study of QCD Radiation in VBF Higgs Production with Vincia and Pythia, SciPost Phys. 12 (2022) 010 [2106.10987].
- [58] J. Cruz-Martinez, S. Forte, N. Laurenti, T. R. Rabemananjara and J. Rojo, LO, NLO, and NNLO parton distributions for LHC event generators, JHEP 09 (2024) 088 [2406.12961].
- [59] A. Buckley, J. Ferrando, S. Lloyd, K. Nordström, B. Page, M. Rüfenacht et al., LHAPDF6: parton density access in the LHC precision era, Eur. Phys. J. C 75 (2015) 132 [1412.7420].
- [60] Particle Data Group collaboration, S. Navas et al., Review of particle physics, Phys. Rev. D 110 (2024) 030001.
- [61] A. Denner, S. Dittmaier, M. Roth and D. Wackeroth, Electroweak radiative corrections to e+ e- —> W W —> 4 fermions in double pole approximation: The RACOONWW approach, Nucl. Phys. B 587 (2000) 67 [hep-ph/0006307].
- [62] P. Nason, MINT: A Computer program for adaptive Monte Carlo integration and generation of unweighted distributions, 0709.2085.
- [63] M. Cacciari, G. P. Salam and G. Soyez, The anti- $k_t$  jet clustering algorithm, JHEP 04 (2008) 063 [0802.1189].
- [64] M. Cacciari, G. P. Salam and G. Soyez, FastJet User Manual, Eur. Phys. J. C 72 (2012) 1896 [1111.6097].
- [65] C. Bittrich, P. Kirchgaeßer, A. Papaefstathiou, S. Plätzer and S. Todt, Soft QCD effects in VBS/VBF topologies, Eur. Phys. J. C 82 (2022) 783 [2110.01623].
- [66] CMS collaboration, A. Hayrapetyan et al., Constraints on the Higgs boson self-coupling from the combination of single and double Higgs boson production in proton-proton collisions at s=13TeV, Phys. Lett. B 861 (2025) 139210 [2407.13554].
- [67] A. Alboteanu, W. Kilian and J. Reuter, Resonances and Unitarity in Weak Boson Scattering at the LHC, JHEP 11 (2008) 010 [0806.4145].

[68] J. Braun, P. Bredt, G. Heinrich and M. Höfer, Double Higgs Production in Vector Boson Fusion at NLO QCD in HEFT, 2502.09132.